Apoptosis inhibitor ARC promotes breast tumorigenesis, metastasis, and chemoresistance

Published in final edited form as:
Cancer Res. 2011 December 15; 71(24): 7705–7715. doi:10.1158/0008-5472.CAN-11-2192.

Apoptosis inhibitor ARC promotes breast tumorigenesis, metastasis and chemoresistance

Christina M. Medina-Ramirez[1,2,5], **Sumanta Goswami**[3,6,7], **Tatiana Smirnova**[3], **Daniel Bamira**[1,5], **Benjamin Benson**[7], **Neal Ferrick**[1,5], **Jeffrey Segall**[3,6], **Jeffrey W. Pollard**[4,6], and **Richard N. Kitsis**[1,2,5,6,8]

[1]Department of Medicine, Albert Einstein College of Medicine, Bronx, NY

[2]Department of Cell Biology, Albert Einstein College of Medicine, Bronx, NY

[3]Department of Anatomy & Structural Biology, Albert Einstein College of Medicine, Bronx, NY

[4]Department of Developmental & Molecular Biology, Albert Einstein College of Medicine, Bronx, NY

[5]Wilf Family Cardiovascular Research Center, Albert Einstein College of Medicine, Bronx, NY

[6]Albert Einstein Cancer Center, Albert Einstein College of Medicine, Bronx, NY

[7]Department of Biology, Yeshiva University, New York, NY

Abstract

ARC (Apoptosis Repressor with Caspase recruitment domain) inhibits both death receptor- and mitochondrial/ER-mediated pathways of apoptosis. While expressed mainly in terminally differentiated cells, ARC is markedly upregulated in a variety of human cancers, where its potential contributions have not yet been defined. In this study, we provide evidence of multiple critical pathophysiological functions for ARC in breast carcinogenesis. In the polyoma middle T-antigen (PyMT) transgenic mouse model of breast cancer, where endogenous ARC is strongly upregulated, deletion of the ARC-encoding gene *nol3* decreased primary tumor burden without affecting tumor onset or multiplicity. More notably, ARC deficiency also limited tumor cell invasion and the number of circulating cancer cells, markedly reducing the number of lung metastases. Conversely, ectopic overexpression of ARC in a PyMT-derived metastatic breast cancer cell line increased invasion *in vitro* and lung metastasis *in vivo*. We confirmed these results in a humanized orthotopic model based on MDA-MB-231-derived LM2 metastatic breast cancer cells, in which RNAi-mediated knockdown of ARC levels was demonstrated to reduce tumor volume, local invasion, and lung metastases. Lastly, we found that endogenous levels of ARC conferred chemoresistance in primary tumors as well as invading cell populations. Our results establish that ARC promotes breast carcinogenesis by driving primary tumor growth, invasion and metastasis as well as by promoting chemoresistance in invasive cells.

Keywords

ARC; breast cancer; metastasis; chemoresistance; cell death

[8]Correspondending author: Richard N. Kitsis, Albert Einstein College of Medicine, Forchheimer G46, 1300 Morris Park Avenue, Bronx, NY 10461, Telephone (718) 430-2609, FAX (718) 430-8989, richard.kitsis@einstein.yu.edu.

Conflicts of interest: None

Supplementary Information: Supplementary Figure Legend and one Supplementary Figure

Introduction

Breast cancer is the second most common cause of cancer deaths in women with mortality attributable to the metastatic spread to vital organs such as lung, liver, and bone (1). Furthermore, the resistance of invasive cells to cancer therapies is a major barrier to patient survival (2). Therefore, an improved understanding of the endogenous factors that mediate tumorigenesis, invasion, metastasis, and treatment resistance is essential for improving outcome. Both promotion of cellular proliferation and suppression of apoptosis are critical for carcinogenesis (3), and proteins that control these processes are often dysregulated (4). Defects in apoptosis have been implicated in multiple aspects of carcinogenesis including the survival of transformed cells, resistance to hypoxia, metastasis, and resistance to various therapeutic agents (3–6).

ARC (Apoptosis Repressor with Caspase Recruitment Domain) is an endogenous inhibitor of apoptosis (7, 8) that has the unusual property of antagonizing both the extrinsic (death receptor) and intrinsic (mitochondrial/ER) pathways (9). We and others have delineated molecular mechanisms that mediate these actions including direct interactions of ARC with (a) Fas, FADD, and procaspase-8, which interfere with DISC assembly (9); (b) Bax, that suppress Bax conformational activation and mitochondrial translocation (9, 10); and (c) p53 that inhibit p53 transcriptional function and nuclear localization (11).

Under normal conditions, ARC is abundant primarily in terminally differentiated cells such as cardiac and skeletal myocytes and neurons (7, 8). ARC expression is strongly upregulated, however, in a wide variety of cancer cell lines (12–16). Moreover, we and others have noted that ARC levels are markedly increased in primary human epithelial cancers including breast, colon, cervical, and ovarian compared with the corresponding normal tissues (12, 13), as well as in acute myelogenous leukemia (AML) (17). Increases in ARC protein levels in some cancers, including breast, are mediated by Ras signaling through both transcriptional activation of *nol3*, the locus encoding ARC, and stabilization of the ARC protein (18). Microarray analyses indicate that ARC expression is a predictor of invasion and metastasis in humans (19, 20), and high ARC levels prognosticate decreased survivorship in glioblastoma multiforme (16) and AML (17). Moreover, manipulation of ARC levels in cancer cell lines has been shown to regulate their sensitivities to various chemotherapies (12, 16, 18, 21, 22).

Although the induction of ARC in human cancers is well established, the functional relevance of this protein to the pathogenesis of any cancer is not known. In this study, we employed a combination of genetically-manipulated mice and xenograft studies to delineate the role of ARC in the pathogenesis of breast cancer from tumor onset through metastasis. The data demonstrate that ARC is a previously unrecognized regulator of multiple aspects of breast carcinogenesis and modulates the sensitivities of both primary tumors and the invading cell population to chemotherapy.

Materials and Methods

Plasmids, viruses, cells

Retrovirus encoding ARC-HA (9) was generated using pBabe-Neo (Addgene) in 293T Phoenix amphotropic packaging cells (ATCC) (23). pLKO.1-puro, containing shRNA sequences targeted to human ARC (3’UTR: TRCN0000118447 (shRNA 47) or coding region: TRCN0000118448 (shRNA 48)) or a control shRNA (Sigma), was used to generate lentivirus in HEK293T cells (23, 24). LM2 (subline 4175) (25) cells (provided by Drs. S. Tavazoie and J. Massagué) and Met-1 cells (26) (provided by Dr. Jeffrey Pollard) were stably transduced with virus using Polybrene 8μg/mL (Sigma), and pools of cells studied.

Cells derived from the provided starting isolates were passaged for no more than 2–3 months. The Met-1 cells were authenticated by Dr. Pollard in the past year by demonstrating continued expression of PyMT and the absence of rejection when transplanted into FVB mice. The LM2 cells have been characterized extensively by Dr. Massague (25).

Generation of PyMT; *nol3*$^{-/-}$ mice

We generated mice with generalized deletion both alleles of *nol3* (encompassing the entire open reading frame of ARC) and backcrossed them onto a C57Bl/6 background as described (27). The absence of ARC protein in hearts of *nol3*$^{-/-}$ mice is shown in Supplementary Fig. S1. These mice were backcrossed 6 times onto an FVB background and then crossed with FVB mice hemizygous for an MMTV-PyMT transgene (28). As shown in Fig. 1, PyMT; *nol3*$^{-/-}$mammary tumors lack ARC protein, while PyMT; *nol3*$^{+/+}$ tumors express it abundantly.

Tissue/protein isolation and western blotting

Cells and tissues were lysed using RIPA buffer with protease inhibitors. Mammary epithelial organoids were isolated as described (18). SDS-PAGE was performed with 20–40μg of protein under reducing conditions and transferred to nitrocellulose membranes (9). Immunoblotting was performed with rabbit polyclonal antisera against ARC (Cayman, 1:2000) and a mouse monoclonal antibody against β-actin (Sigma, 1:10,000), and analyzed with a Li-Cor Odyssey system.

Immunohistochemistry and histological analyses

Tissues were fixed in 10% neutral buffered formalin and immunohistochemistry performed as described (18) using the ARC antisera (Cayman, 1:500) or a mouse monoclonal antibody against Ki67 (Novocastra,1:200), and counterstained with hematoxylin. TUNEL was performed using ApopTag®Plus *In Situ* Apoptosis Detection Kit (Chemicon). Lung metastases were analyzed using 6 sections spaced at 300 μM from a whole embedded lung and stained with hematoxylin & eosin (PyMT mice and Met-1 tail vein injections) or vimentin (Novocastra 1:500) (LM2 xenograft model). Images of stained slides were obtained with a Nikon Eclipse TE2000-S microscope and Spot R/T CCD camera.

Invasion and blood burden assays

In vitro invasion assay was performed as described with BD BioCoat Matrigel Invasion Chambers (BD 354480) using 2.5×10^4 Met-1 cells and 10% FBS as chemoattractant over a 22 hour incubation. *In vivo* invasion assay was performed as described (29) with EGF (25 nM) used as chemoattractant. Cells were collected for 4 h, stained with DAPI, and counted (29). Blood burden was assessed as described (30) and tumor cell colonies from blood were grown in 20% FBS/DMEM media and counted 7 days after plating.

Met-1 tail vein injections and LM2 xenograft model

Experimental metastasis was assessed by injecting 0.5×10^6 mouse Met-1 cells suspended in 300μl of sterile PBS in the tail vein of 8 week old female FVB mice, and lung metastases analyzed 14 d later as described above. Mammary xenografts were produced by injecting human LM2 cells stably expressing luciferase (1×10^6 cells in 100μl of sterile PBS containing 20% rat tail collagen (BD)) into the lower right mammary gland of 6 w old female SCID mice (National Cancer Institute). Tumor volume was determined by caliper measurements ($0.5 \times \text{length} \times \text{width}^2$) or bioluminescence imaging. Spontaneous lung metastases were scored 8 w post-injection as above.

In vivo bioluminescence imagining and analysis

Mice with xenografts were injected with D-luciferin potassium salt (150 mg/kg ip, Caliper Life Sciences) for tumor detection or VivoGlo Caspase-3/7 Substrate (z-DEVD-Aminoluciferin sodium salt, 50 mg/kg ip, Promega,) for apoptosis detection. Anesthetized mice were imaged 12–15 minutes after injection using the Xenogen IVISR 200 series system with *Living Image* software (Caliper Life Sciences) for acquisition and analysis. Bioluminescence intensity plots are quantified as photon flux ($p/sec/cm^2/sr$) for the region of interest (ROI) as selected by the auto ROI tool.

Chemosensitivity assays

LM2 cells were plated at a density of 700 cells/mm^2 and treated with indicated doses of doxorubicin (Sigma) for 24 h. Cell death was quantified with calcein AM/ethidium bromide (Sigma) and counterstaining with Hoechst 33342 (10 μg/ml, Invitrogen) as described (31). SCID mice bearing LM2 mammary xenografts were injected with doxorubicin 5mg/kg when tumors reached a volume of ~100 cm^3 (calipers), and apoptosis analyzed 72 hours post-injection by bioluminescence as above. The chemosensitivity of the invading cell population, captured from PyMT mice using the *in vivo* invasion assay above, was determined as described (32). Cells were cultured overnight, and sensitivities to 3 h treatments with doxorubicin (5 μM) or tamoxifen (5 μM, Sigma) assessed using FACS analysis of Annexin V/7-AAD stained cells (Guava Technologies). Cells positive for Annexin V or double positive for Annexin V and 7-AAD were considered dead.

Statistical analyses

Data are expressed as mean ± SEM. Differences were determined using Student's unpaired two-tailed *t* test (2 groups) or ANOVA with Bonferroni post-test (≥ 3 groups) using Prism 5 (GraphPad Software). $P < 0.05$ was considered significant.

Results

ARC expression is induced in mammary tumors of PyMT mice

We have previously demonstrated that ARC is abundant in primary human breast cancers, but absent or expressed at very low levels in normal breast tissue (12). Our initial approach to assessing the functional importance of ARC in breast carcinogenesis was to employ mice hemizygous for a polyoma middle T-antigen (PyMT) transgene expressed in the mammary epithelium under the control of mouse mammary tumor virus (MMTV) long terminal repeats (hereafter referred to as PyMT mice) (28). The PyMT model is highly penetrant and replicates critical aspects of the human disease including progression from primary tumors to metastases (33). The rationale for selecting an aggressive model was to provide an especially challenging target for subsequent rescue experiments. To determine if this is a suitable model in which to study the effects of ARC on mammary carcinogenesis, we first assessed whether ARC expression is induced in PyMT mice. Transgenic expression of PyMT markedly increased the abundance of ARC protein in mammary tumors of various stages, including adenomas/mammary intraepithelial neoplasia (MIN) and invasive carcinoma, compared with non-transgenic mice (Fig. 1A, top row). ARC expression was evident in each tumor of each PyMT mouse, although intensity of immunostaining varied mildly among tumors. The specificity of the antisera is indicated by the absence of ARC immunostaining in PyMT mice in which both *nol3* alleles were deleted (Fig. 1A, bottom row). Similar results were evident by Western blotting (Fig. 1B). Interestingly, ARC expression persisted in metastases dissected from lung tissue (Fig. 1C). These data demonstrate that ARC expression is induced in early tumors to metastases of PyMT mice, suggesting that ARC may be involved in multiple stages of mammary carcinogenesis.

Endogenous ARC promotes tumor burden, but does not affect tumor onset or multiplicity

To assess the role of ARC in mammary carcinogenesis, we employed mice with generalized deletion of both *nol3* alleles. In the absence of a PyMT transgene, *nol3* null mice demonstrated no baseline abnormalities and, specifically, exhibited no mammary pathology (not shown). When hemizygous for an MMTV-PyMT transgene, *nol3* null mice were born in Mendelian proportions and without detectable abnormalities. Mammary tumors first became palpable in both PyMT; $nol3^{+/+}$ and PyMT; $nol3^{-/-}$ mice at 7 w of age (P NS), and by 10 w of age, 100% of mice of each genotype exhibit at least one tumor (Fig. 2A). Thus, the presence of ARC does not influence tumor onset. Similarly, tumor multiplicity was not affected by ARC (Fig. 2B). In contrast, tumor burden, the wet weight of all excised tumors, differed markedly between PyMT; $nol3^{+/+}$ and PyMT; $nol3^{-/-}$ mice. While differences were not yet evident at 12 w, deletion of *nol3* reduced tumor burden 34% (9.41 ± 0.78 g in PyMT; $nol3^{+/+}$ mice versus 6.19 ± 0.48 g in PyMT; $nol3^{-/-}$ mice; $P < 0.0001$) at 14 w when tumor size is at the maximum acceptable limit (Fig. 2C). Thus, endogenous levels of ARC promote increases in tumor burden, which likely reflect increases in individual tumor mass because tumor multiplicity is unchanged.

Endogenous ARC promotes tumorigenesis through increased proliferation rather than decreased apoptosis

To determine the mechanisms by which ARC increases tumor burden in PyMT mice, we analyzed mammary tumors for apoptosis and proliferation at 14 w of age. The difference in the number of TUNEL-positive tumor cells per field between PyMT; $nol3^{+/+}$ and PyMT; $nol3^{-/-}$ mice was not statistically significant despite studying 8–10 mice of each genotype (15.4 ± 1.3 cells per field in PyMT; $nol3^{+/+}$ versus 17.2 ± 1.3 in PyMT; $nol3^{-/-}$; P NS) (Fig. 2D). While this is surprising in light of the established role of ARC as an apoptosis inhibitor, it indicates that differences in apoptosis rates do not account for effects on tumor burden. In contrast, cellular proliferation, as measured by Ki67 staining, was 44% lower in PyMT; $nol3^{-/-}$, as compared with PyMT; $nol3^{+/+}$, mice(356.9 ± 20.8 in PyMT; $nol3^{+/+}$ miceversus 201.2 ± 20.0 in PyMT; $nol3^{-/-}$ mice; $P < 0.0001$) (Fig. 2E). These data indicate that endogenous levels of ARC promote proliferation of mammary cancer cells *in vivo*, thereby contributing to increased tumor burden.

Endogenous ARC promotes invasion and metastasis

The high frequency with which primary mammary tumors metastasize in the PyMT model allowed us to evaluate the effect of ARC on invasion and metastasis. We first determined whether ARC influences local invasion *in vivo* by assessing the abilities of tumor cells to gain access into needles containing Matrigel that had been permeated with EGF as a chemoattractant. The needles were inserted directly into the primary mammary tumors. Needles in tumors of PyMT; $nol3^{-/-}$ mice captured 44% less cells than those in tumors of PyMT; $nol3^{+/+}$ mice (716.0 ± 69.3 cells per needle in PyMT; $nol3^{+/+}$ mice versus 399.0 ± 57.7 in PyMT; $nol3^{-/-}$ mice; $P < 0.05$) (Fig. 3A). These data indicate that ARC promotes local invasion *in vivo*, a key step in metastatic progression.

Following invasion, tumor cells may gain access to blood or lymph by intravasating into blood vessels or lymphatics, a prelude to distant metastasis. The concentration of tumor cells in blood or lymph reflects rates of intravasation minus extravasation. Accordingly, we next assessed the concentration of tumor cells circulating in the blood or blood burden. The blood burden of PyMT; $nol3^{-/-}$ mice was 40% lower than that of PyMT; $nol3^{+/+}$ mice (927.3 ± 105.5 colonies per ml blood in PyMT; $nol3^{+/+}$ mice versus 560.3 ± 118.6 in PyMT; $nol3^{-/-}$ mice; $P < 0.05$) (Fig. 3B). Differences in plating efficiencies were excluded using primary tumor cells from the two genotypes (not shown).

To assess the effect of ARC on the onset and number of lung metastases, we analyzed hematoxylin & eosin-stained sections. Metastases were not detectable in either genotype at 10 w of age. At 12 w, 6/14 PyMT; *nol3*$^{+/+}$ mice and 5/11 PyMT; *nol3*$^{-/-}$ mice contained at least one lung metastasis (P NS), indicating similar times of initiation of metastasis in both genotypes. At 14 w, 100% of the mice in both groups exhibited at least one detectable lung metastasis. Importantly, however, the number of lung metastases was 44% lower in PyMT; *nol3*$^{-/-}$, as compared with PyMT; *nol3*$^{+/+}$, mice (12.0 ± 1.6 in PyMT; *nol3*$^{+/+}$ versus 7.0 ± 1.7 in PyMT; *nol3*$^{-/-}$mice; $P < 0.05$) (Fig. 3C, left graph). Even following normalization to tumor burden, the number of metastases remains significantly reduced in the mice with *nol3* deletion ($P < 0.01$) (Fig. 3C, right graph). These data indicate that endogenous levels of ARC facilitate lung metastasis.

Converse effects from ARC overexpression

The above experiments assessed effects of ARC absence. Conversely, we wished to evaluate the effect of ARC overexpression. Met-1 cells are a metastatic mouse mammary tumor cell line derived from PyMT mice (26). Despite our demonstration of ARC expression in lung metastases from PyMT mammary tumors *in vivo* (Fig. 1C), the Met-1 line does not contain endogenous ARC, making them suitable for gain of function studies. Accordingly, we generated Met-1 cells with stable with overexpression of ARC (Fig. 3D). In light of our results showing a significant effect of ARC deletion on invasion *in vivo*, we first tested ARC-overexpressing Met-1 cells in an *in vitro* invasion assay. Using a modified Boyden chamber assay (34) with Matrigel as the barrier, Met-1 cells expressing exogenous ARC demonstrated 64% more invasion than cells transduced with empty vector (24.7 ± 4.5 cells per field in vector-transduced cells versus 40.6 ± 5.8 ARC-transduced cells; $P < 0.05$) (Fig. 3E). Statistically significant differences were not obtained in the absence of Matrigel indicating that the observed effects likely reflect invasion rather than motility (not shown).

To assess whether ARC overexpression facilitates lung metastasis, we employed tail vein injection assays, which bypass the local invasion and intravasation steps required for spontaneous metastasis in the PyMT model. When injected into the tail vein of syngeneic wild type FVB female mice, Met-1 cells overexpressing ARC resulted in 1.7-fold more lung metastases than did the vector control group (53.8 ± 9.1 in mice injected with vector control-transfected cells versus 92.1 ± 9.6 in mice receiving in ARC-overexpressing cells; $P < 0.01$) (Fig. 3F). Thus, ARC overexpression in Met-1 cells promotes post-intravasation metastatic efficiency.

Endogenous ARC promotes tumorigenesis, invasion, and metastasis in a humanized model of breast cancer

To test our findings in a humanized breast cancer model, we employed human LM2 cells, a subset of MDA-MB-231 cells that have a tropism to metastasize to lung (25). Our approach was to knock down ARC in these cells, xenograft them into the mammary glands of SCID mice, and assess tumorigenesis, invasion, and metastasis. In contrast to the generalized knockout of *nol3* studied earlier, this model also allows us to assess whether the various phenotypes result from deficiency of ARC specifically in breast cancer cells.

ARC levels were reduced using lentiviral transduction of different shRNAs (Fig. 4A). ARC shRNA 48, which results in 72% knockdown in ARC levels (Fig. 4A), reduces xenograft tumor volume most markedly (Fig. 4B). At 9 w post-transplantation, volume of tumors derived from ARC shRNA 48-expresssing cells is decreased 42% compared with those expressing control shRNA (2475 ± 217 mm^3 with control shRNA versus 1428 ± 142 mm^3 with ARC shRNA 48; $P < 0.0001$). ARC shRNA 47, which decreases ARC levels less dramatically (57%) (Fig. 4A), results in an intermediate decrease in tumor volume, although

statistical significance was not achieved (Fig. 4B). We wished to detect ARC-dependent changes in tumor volume at even earlier time points when caliper measurements are not feasible. As the LM2 cells have been engineered to express luciferase, we detected ARC-dependent differences in tumor volume using bioluminescence. Compared with transplanted cells expressing control shRNA, those expressing ARC shRNA 48 exhibit markedly smaller tumors at 3 w post-transplantation ($9.86 \times 10^9 \pm 1.01 \times 10^9$ p/s/r/cm^2/sr (photon flux) with control shRNA versus $3.46 \times 10^9 \pm 3.05 \times 10^8$ with ARC shRNA 48; $P < 0.001$), a finding that is suggested even at 2 w, although statistical significance is not yet present at this time point (Fig. 4C).

We next assessed local invasion from LM2 tumors using the *in vivo* invasion assay. ARC knockdown resulted in 64% less invading cells (407.3 ± 18.1 cells/needle with control shRNA versus 148.2 ± 10.4 with ARC shRNA 48; $P < 0.0001$) (Fig. 4D). Mice were also monitored for spontaneous lung metastases as assessed by immunostaining with an antibody specific for human vimentin. At 8 w post-transplantation, the number of lung metastases was 62% less in mice receiving LM2 cells with ARC knockdown (419.7 ± 100.1 metastases per section with control shRNA versus 157.8 ± 63.6 with ARC shRNA 48; $P < 0.05$) (Fig. 4E).

Thus, as in PyMT mice (Figs. 2C, 3A, 3C), these data show that endogenous levels of ARC promote increased tumor volume, local invasion, and metastasis in a humanized model of breast cancer. Moreover, cell autonomous mechanisms are sufficient to account for this effect.

Endogenous ARC confers chemoresistance to tumors and invading cell population

We next determined whether ARC affects the susceptibility of primary mammary tumors and the invading cell population to chemotherapy. Cultured LM2 cells with ARC knockdown were more sensitive to killing by doxorubicin than controls (Fig. 5A). To assess potential effects of ARC on the susceptibility of primary tumors to chemotherapy *in vivo*, we measured the apoptotic response of LM2 tumors to doxorubicin. This was accomplished with bioluminescence using z-DEVD-aminoluciferin, which requires cleavage by caspases-3/7 to function as a luciferase substrate. ARC knockdown dramatically potentiated the apoptotic response of tumors to doxorubicin (Fig. 5B, bars 3 and 4; $P < 0.05$). Moreover, while tumors deficient in ARC responded to doxorubicin (Fig. 5B, bars 2 and 4; $P < 0.05$), control tumors exhibited no significant changes in apoptosis following treatment (Fig. 5B, bars 1 and 3; P NS). These data indicate that endogenous levels of ARC confer chemoresistance to primary tumors.

The ability of primary tumor cells to invade locally is an important factor in the development of distant metastases, and the invading cell population is known to be more chemoresistant than primary tumor cells (32). Accordingly, using the PyMT model, we exploited the *in vivo* invasion assay to capture locally invading cells, enabling us to assess the effect of ARC on their resistance to chemotherapy. Deletion of *nol3* markedly augmented killing by doxorubicin ($P < 0.05$) (Fig. 5C) and tamoxifen ($P < 0.001$) (Fig. 5D). We conclude that endogenous levels of ARC contribute to chemoresistance of the invading cell population.

Discussion

These results indicate that ARC, previously recognized as a regulator of cell death solely in terminally differentiated cells (e.g. cardiac myocytes), promotes multiple aspects of breast carcinogenesis. This conclusion is supported by experiments in both genetically manipulated mice and xenografts of human breast cancer cells. Importantly, our studies emphasize genetic loss of function to provide insight into the importance of endogenous ARC levels.

Our previous discovery that ARC abundance is markedly increased in human breast cancers is recapitulated in mammary tumors of MMTV-PyMT transgenic mice (Fig. 1). Based on prior studies (18), we presume that ARC levels are increased, in part, through upregulation of Ras signaling by the PyMT transgene (35). The persistence of ARC from primary tumors through metastases in this model is in accordance with our results demonstrating involvement of ARC in pathogenesis at multiple stages. In fact, ARC expression is even higher in the invading cell population than in corresponding primary mammary tumors of PyMT mice (unpublished data, S. Goswami and J. Condeelis).

Onset and multiplicity of PyMT tumors are unaffected by the loss of ARC suggesting that ARC is not necessary for tumor initiation. Rather, our data indicate that ARC strongly influences tumor growth (Fig. 2C). Despite its known function as an apoptosis inhibitor, the absence of ARC does not significantly increase apoptosis in this system (Fig. 2D). Although the explanation for this is not clear, we hypothesize the presence of redundant cell death inhibitors. Surprisingly, the absence of ARC reduces cellular proliferation (Fig. 2E). This proliferation function of ARC has not been previously described, although we have recently observed that ARC knockdown/knockout also impairs the proliferation of benign MCF-10A breast epithelial cells (unpublished data, C. Medina-Ramirez and R. Kitsis) and hypoxic pulmonary arterial smooth muscle cells *in vivo* (27). The mechanism of ARC-induced cellular proliferation is not known. While the ability of ARC to inactivate p53 may be involved (11), this explanation is less likely in PyMT tumors in which activated Akt (35) would be predicted to have already decreased p53 levels through MDM2-mediated degradation (36).

ARC does not influence the kinetics with which lung metastases develop in the PyMT model. Rather, the number of lung metastases in PyMT mice lacking ARC is markedly reduced suggesting decreases in the efficiency of this process. The mechanisms by which ARC affects invasion and metastasis appear complex. Absence of ARC reduces local invasion, blood burden (reflecting the balance between intravasation and extravasation), and metastasis by similar amounts (40–44%) (Fig. 3A, B, C), implying that the most proximal event, invasion, may play the rate-limiting role. Of note, significant effects of ARC on invasion were observed in all systems studied (PyMT (Fig. 3A), met-1 (Fig. 3E), and LM2 (Fig. 4D)). While the mechanisms by which ARC facilitates invasion are unclear, emerging evidence suggests that other cell death regulators (e.g., procaspase-8, IAPs, Bcl-2) may promote invasion by effects independent of their apoptosis functions (37–41). Procaspase-8, in particular, promotes migration and metastasis through interactions with a focal adhesion kinase (FAK) complex (40, 41). Since ARC and procaspase-8 interact (8, 9) we tested the possibility that the effects of ARC on invasion involve procaspase-8, but found no evidence in support of this model (K. Bacos and D. Stupack, not shown). In addition to the effects of ARC on invasion, administration of cancer cells by tail vein to bypass invasion and intravasation steps still demonstrates that ARC increases the efficiency of lung metastasis (Fig. 3F). A large proportion of injected cells are known to die rapidly in the circulation and/or the lung parenchyma (42). This lack of persistence limits the ability of these cells to form macrometastases. Accordingly, it is likely that ARC confers a post-intravasation survival advantage that increases the efficiency lung metastasis. These data suggest that ARC regulates invasion and metastasis at multiple steps.

The effects of ARC on tumor growth, invasion and metastasis observed in the PyMT model were reproduced using LM2 xenografts (Fig. 4). The significance of this is two-fold. First, these experiments translate our findings in mouse cells to a humanized model of breast cancer. Second, these data indicate that ARC exerts cell autonomous effects in mammary carcinogenesis, a conclusion that could not be drawn from PyMT mice that lack ARC in non-tumor, as well as, tumor cells.

We have shown that ARC confers resistance to killing by doxorubicin using human Hs578T (12) and LM2 (Fig. 5A) cells. The LM2 xenografts provide a useful preclinical model to test the contributions of ARC to chemoresistance *in vivo*. Endogenous levels of ARC by themselves are sufficient to render cells of the primary tumor resistant to doxorubicin-induced death (Fig. 5B). In this situation, the anti-apoptosis function of ARC is clearly involved. The increased chemoresistance of the invading cell population (32) poses an particularly challenging barrier to effective treatment. Our experiments, in which cells captured in the process of invading are tested for their sensitivities to doxorubicin and tamoxifen, demonstrate that ARC is a critical factor in the chemoresistance of this population (Fig 5C, D).

In conclusion, ARC promotes multiple aspects of breast carcinogenesis including tumorigenesis, invasion, metastasis, and chemoresistance. Given these multiple roles, ARC may provide a particularly potent target for future therapies directed against breast cancer.

Supplementary Material

Refer to Web version on PubMed Central for supplementary material.

Acknowledgments

We are grateful for the assistance and advice of Min Zheng, Dr. Chang-Fu Peng, Harry Hou, Robert J. Faigen, Dayle Hodge, Binzhi Qian, Fred Bauzon, and Drs. Isabelle Mercier and Rani Sellers. We acknowledge Dr. Joan S. Brugge for advice and early encouragement, and Drs. John Condeelis, Rachel Hazan, and Dwayne Stupack for discussions and insights. We thank Drs. Sohail Tavazoie and Joan Massagué for LM2 cells.

Grant Support

This work was supported by 5R01HL060665 (RNK), 5P01CA100324 (SG), 5P30CA013330, Breast Cancer Alliance Young Investigator Award (SG), The Ford Foundation Diversity Pre-doctoral Fellowship (CMM-R), and the Dr. Gerald and Myra Dorros Chair of the Albert Einstein College of Medicine (RNK). We are grateful to the Wilf Family for their ongoing support.

References

1. Weigelt B, Peterse JL, van ’t Veer LJ. Breast cancer metastasis: markers and models. Nat Rev Cancer. 2005; 5:591–602. [PubMed: 16056258]
2. Igney FH, Krammer PH. Death and anti-death: tumour resistance to apoptosis. Nat Rev Cancer. 2002; 2:277–88. [PubMed: 12001989]
3. Hanahan D, Weinberg RA. The hallmarks of cancer. Cell. 2000; 100:57–70. [PubMed: 10647931]
4. Letai AG. Diagnosing and exploiting cancer’s addiction to blocks in apoptosis. Nat Rev Cancer. 2008; 8:121–32. [PubMed: 18202696]
5. Mehlen P, Puisieux A. Metastasis: a question of life or death. Nat Rev Cancer. 2006; 6:449–58. [PubMed: 16723991]
6. Wyllie AH, Bellamy CO, Bubb VJ, Clarke AR, Corbet S, Curtis L, et al. Apoptosis and carcinogenesis. Br J Cancer. 1999; 80 (Suppl 1):34–7. [PubMed: 10466759]
7. Geertman R, McMahon A, Sabban EL. Cloning and characterization of cDNAs for novel proteins with glutamic acid-proline dipeptide tandem repeats. Biochim Biophys Acta. 1996; 1306:147–52. [PubMed: 8634331]
8. Koseki T, Inohara N, Chen S, Nunez G. ARC, an inhibitor of apoptosis expressed in skeletal muscle and heart that interacts selectively with caspases. Proc Natl Acad Sci U S A. 1998; 95:5156–60. [PubMed: 9560245]
9. Nam YJ, Mani K, Ashton AW, Peng CF, Krishnamurthy B, Hayakawa Y, et al. Inhibition of both the extrinsic and intrinsic death pathways through nonhomotypic death-fold interactions. Mol Cell. 2004; 15:901–12. [PubMed: 15383280]

10. Gustafsson AB, Tsai JG, Logue SE, Crow MT, Gottlieb RA. Apoptosis repressor with caspase recruitment domain protects against cell death by interfering with Bax activation. J Biol Chem. 2004; 279:21233–8. [PubMed: 15004034]
11. Foo RS, Nam YJ, Ostreicher MJ, Metzl MD, Whelan RS, Peng CF, et al. Regulation of p53 tetramerization and nuclear export by ARC. Proc Natl Acad Sci U S A. 2007; 104:20826–31. [PubMed: 18087040]
12. Mercier I, Vuolo M, Madan R, Xue X, Levalley AJ, Ashton AW, et al. ARC, an apoptosis suppressor limited to terminally differentiated cells, is induced in human breast cancer and confers chemo- and radiation-resistance. Cell Death Differ. 2005; 12:682–6. [PubMed: 15861191]
13. Mercier I, Vuolo M, Jasmin JF, Medina CM, Williams M, Mariadason JM, et al. ARC (apoptosis repressor with caspase recruitment domain) is a novel marker of human colon cancer. Cell Cycle. 2008; 7:1640–7. [PubMed: 18469522]
14. Zhang YQ, Herman B. Expression and modification of ARC (apoptosis repressor with a CARD domain) is distinctly regulated by oxidative stress in cancer cells. J Cell Biochem. 2008; 104:818–25. [PubMed: 18172857]
15. Wang M, Qanungo S, Crow MT, Watanabe M, Nieminen AL. Apoptosis repressor with caspase recruitment domain (ARC) is expressed in cancer cells and localizes to nuclei. FEBS Lett. 2005; 579:2411–5. [PubMed: 15848180]
16. Ziegler DS, Wright RD, Kesari S, Lemieux ME, Tran MA, Jain M, et al. Resistance of human glioblastoma multiforme cells to growth factor inhibitors is overcome by blockade of inhibitor of apoptosis proteins. J Clin Invest. 2008; 118:3109–22. [PubMed: 18677408]
17. Carter BZ, Qiu YH, Zhang N, Coombes KR, Mak DH, Thomas DA, et al. Expression of ARC (apoptosis repressor with caspase recruitment domain), an antiapoptotic protein, is strongly prognostic in AML. Blood. 2011; 117:780–7. [PubMed: 21041716]
18. Wu L, Nam YJ, Kung G, Crow MT, Kitsis RN. Induction of the apoptosis inhibitor ARC by Ras in human cancers. J Biol Chem. 2010; 285:19235–45. [PubMed: 20392691]
19. Tamoto E, Tada M, Murakawa K, Takada M, Shindo G, Teramoto K, et al. Gene-expression profile changes correlated with tumor progression and lymph node metastasis in esophageal cancer. Clin Cancer Res. 2004; 10:3629–38. [PubMed: 15173069]
20. Takata O, Kawamura YJ, Konishi F, Sasaki J, Kai T, Miyakura Y, et al. cDNA array analysis for prediction of hepatic metastasis of colorectal carcinoma. Surg Today. 2006; 36:608–14. [PubMed: 16794795]
21. Chen LH, Jiang CC, Watts R, Thorne RF, Kiejda KA, Zhang XD, et al. Inhibition of endoplasmic reticulum stress-induced apoptosis of melanoma cells by the ARC protein. Cancer Res. 2008; 68:834–42. [PubMed: 18245485]
22. Wang JX, Li Q, Li PF. Apoptosis repressor with caspase recruitment domain contributes to chemotherapy resistance by abolishing mitochondrial fission mediated by dynamin-related protein-1. Cancer Res. 2009; 69:492–500. [PubMed: 19147562]
23. Swift S, Lorens J, Achacoso P, Nolan GP. Rapid production of retroviruses for efficient gene delivery to mammalian cells using 293T cell-based systems. Curr Protoc Immunol. 2001; Chapter 10(Unit 10):7C.
24. Choe KS, Ujhelly O, Wontakal SN, Skoultchi AI. PU.1 directly regulates cdk6 gene expression, linking the cell proliferation and differentiation programs in erythroid cells. J Biol Chem. 2010; 285:3044–52. [PubMed: 19955566]
25. Minn AJ, Gupta GP, Siegel PM, Bos PD, Shu W, Giri DD, et al. Genes that mediate breast cancer metastasis to lung. Nature. 2005; 436:518–24. [PubMed: 16049480]
26. Borowsky AD, Namba R, Young LJ, Hunter KW, Hodgson JG, Tepper CG, et al. Syngeneic mouse mammary carcinoma cell lines: two closely related cell lines with divergent metastatic behavior. Clin Exp Metastasis. 2005; 22:47–59. [PubMed: 16132578]
27. Zaiman A, Damico R, Thoms-Chesley A, Files D, Kesari P, Johnston L, et al. A Critical Role for the Protein Apoptosis Repressor with Caspase Recruitment Domain in Hypoxia-Induced Pulmonary Hypertension. Circulation. 2011; 124:2533–2542. [PubMed: 22082675]

28. Guy CT, Cardiff RD, Muller WJ. Induction of mammary tumors by expression of polyomavirus middle T oncogene: a transgenic mouse model for metastatic disease. Mol Cell Biol. 1992; 12:954–61. [PubMed: 1312220]
29. Hernandez L, Smirnova T, Wyckoff J, Condeelis J, Segall JE. In vivo assay for tumor cell invasion. Methods Mol Biol. 2009; 571:227–38. [PubMed: 19763970]
30. Xue C, Wyckoff J, Liang F, Sidani M, Violini S, Tsai KL, et al. Epidermal growth factor receptor overexpression results in increased tumor cell motility in vivo coordinately with enhanced intravasation and metastasis. Cancer Res. 2006; 66:192–7. [PubMed: 16397232]
31. Debnath J, Muthuswamy SK, Brugge JS. Morphogenesis and oncogenesis of MCF-10A mammary epithelial acini grown in three-dimensional basement membrane cultures. Methods. 2003; 30:256–68. [PubMed: 12798140]
32. Goswami S, Wang WG, Wyckoff JB, Condeelis JS. Breast cancer cells isolated by chemotaxis from primary tumors show increased survival and resistance chemotherapy. Cancer Research. 2004; 64:7664–7. [PubMed: 15520165]
33. Lin EY, Jones JG, Li P, Zhu L, Whitney KD, Muller WJ, et al. Progression to malignancy in the polyoma middle T oncoprotein mouse breast cancer model provides a reliable model for human diseases. Am J Pathol. 2003; 163:2113–26. [PubMed: 14578209]
34. Albini A. Tumor and endothelial cell invasion of basement membranes. The matrigel chemoinvasion assay as a tool for dissecting molecular mechanisms. Pathol Oncol Res. 1998; 4:230–41. [PubMed: 9761943]
35. Fluck MM, Schaffhausen BS. Lessons in signaling and tumorigenesis from polyomavirus middle T antigen. Microbiol Mol Biol Rev. 2009; 73:542–63. [PubMed: 19721090]
36. Ogawara Y, Kishishita S, Obata T, Isazawa Y, Suzuki T, Tanaka K, et al. Akt enhances Mdm2-mediated ubiquitination and degradation of p53. J Biol Chem. 2002; 277:21843–50. [PubMed: 11923280]
37. Choi J, Choi K, Benveniste EN, Rho SB, Hong YS, Lee JH, et al. Bcl-2 promotes invasion and lung metastasis by inducing matrix metalloproteinase-2. Cancer Res. 2005; 65:5554–60. [PubMed: 15994927]
38. Zuo J, Ishikawa T, Boutros S, Xiao Z, Humtsoe JO, Kramer RH. Bcl-2 overexpression induces a partial epithelial to mesenchymal transition and promotes squamous carcinoma cell invasion and metastasis. Mol Cancer Res. 2010; 8:170–82. [PubMed: 20145039]
39. Mehrotra S, Languino LR, Raskett CM, Mercurio AM, Dohi T, Altieri DC. IAP regulation of metastasis. Cancer Cell. 2010; 17:53–64. [PubMed: 20129247]
40. Barbero S, Barila D, Mielgo A, Stagni V, Clair K, Stupack D. Identification of a critical tyrosine residue in caspase 8 that promotes cell migration. J Biol Chem. 2008; 283:13031–4. [PubMed: 18216014]
41. Barbero S, Mielgo A, Torres V, Teitz T, Shields DJ, Mikolon D, et al. Caspase-8 association with the focal adhesion complex promotes tumor cell migration and metastasis. Cancer Res. 2009; 69:3755–63. [PubMed: 19383910]
42. Wong CW, Lee A, Shientag L, Yu J, Dong Y, Kao G, et al. Apoptosis: an early event in metastatic inefficiency. Cancer Res. 2001; 61:333–8. [PubMed: 11196183]

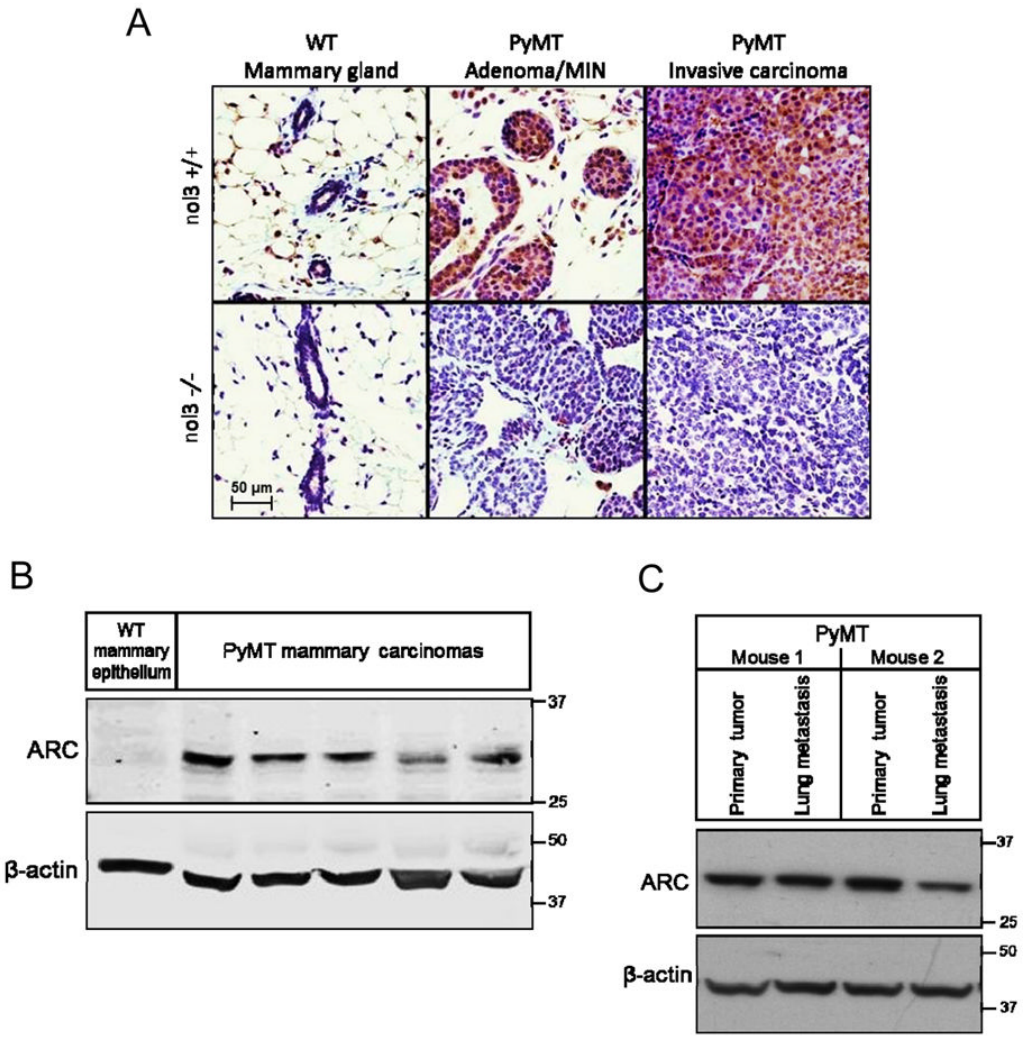

Figure 1.

ARC protein expression in PyMT tumors. *(A)* Immunohistochemical staining for ARC (brown) with hematoxylin counterstain (nuclei, blue) in 8–14 w old virgin female FVB mice of the indicated genotypes. *(B)* Western blot analysis of ARC in epithelium isolated from WT mammary glands and from PyMT mammary carcinomas (5 different mice). *(C)* Western blot analysis of ARC in paired mammary tumor and dissected macroscopic lung metastasis from the same mice.

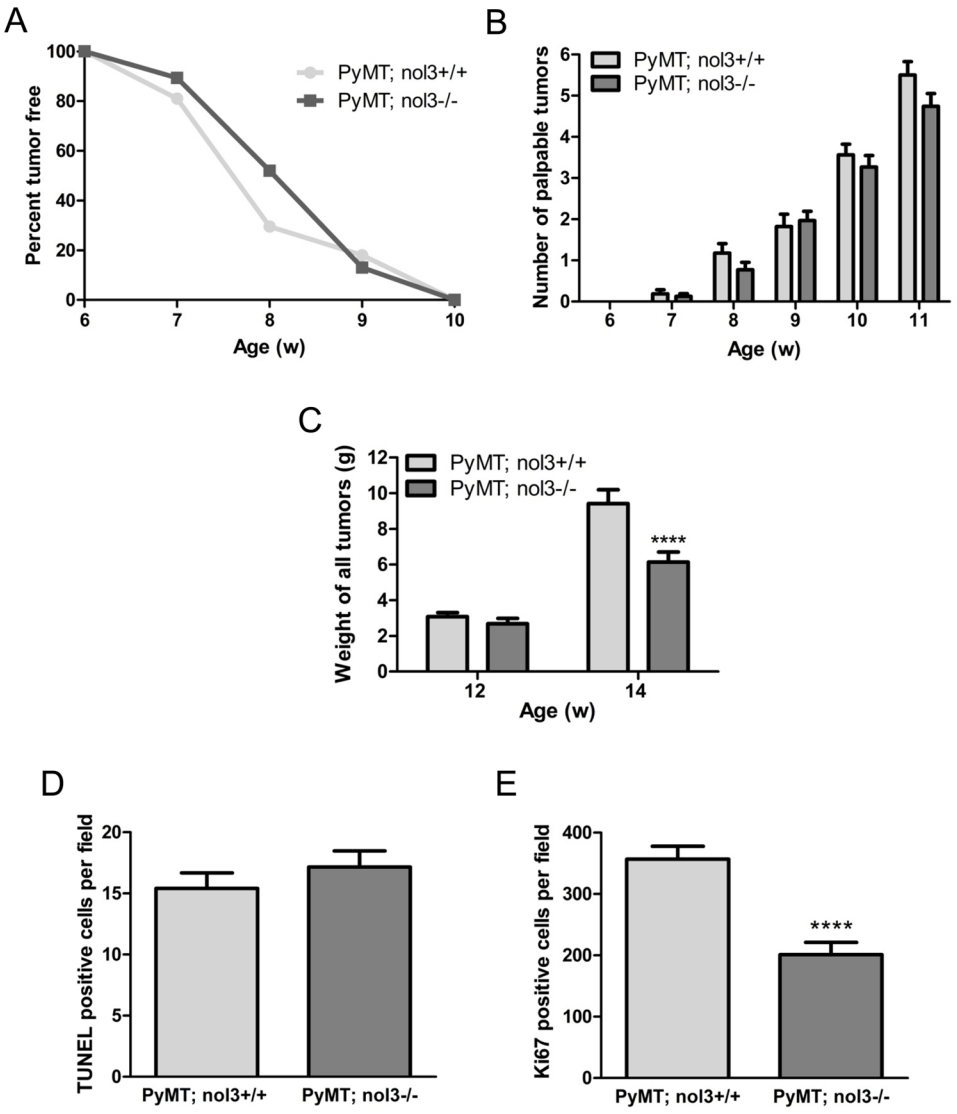

Figure 2.

Absence of ARC reduces mammary tumor burden in PyMT mice by reducing cellular proliferation. *(A)* Tumor onset. *(B)* Tumor multiplicity. (For (*A*) and (*B*), n = 17 *nol3*$^{+/+}$ and 31 *nol3*$^{-/-}$ mice). *(C)* Tumor burden. (12 w: n= 28 *nol3*$^{+/+}$ and 25 *nol3*$^{-/-}$ mice; 14 w: n = 22 *nol3*$^{+/+}$ and 26 *nol3*$^{-/-}$ mice). *(D)* TUNEL. (E) Ki67 staining. (For (*D*) and (*E*), n = 10 *nol3*$^{+/+}$ and 8 *nol3*$^{-/-}$14 w old mice, with ≥ 10 fields (200X) scored per mouse). P values: ****< 0.0001.

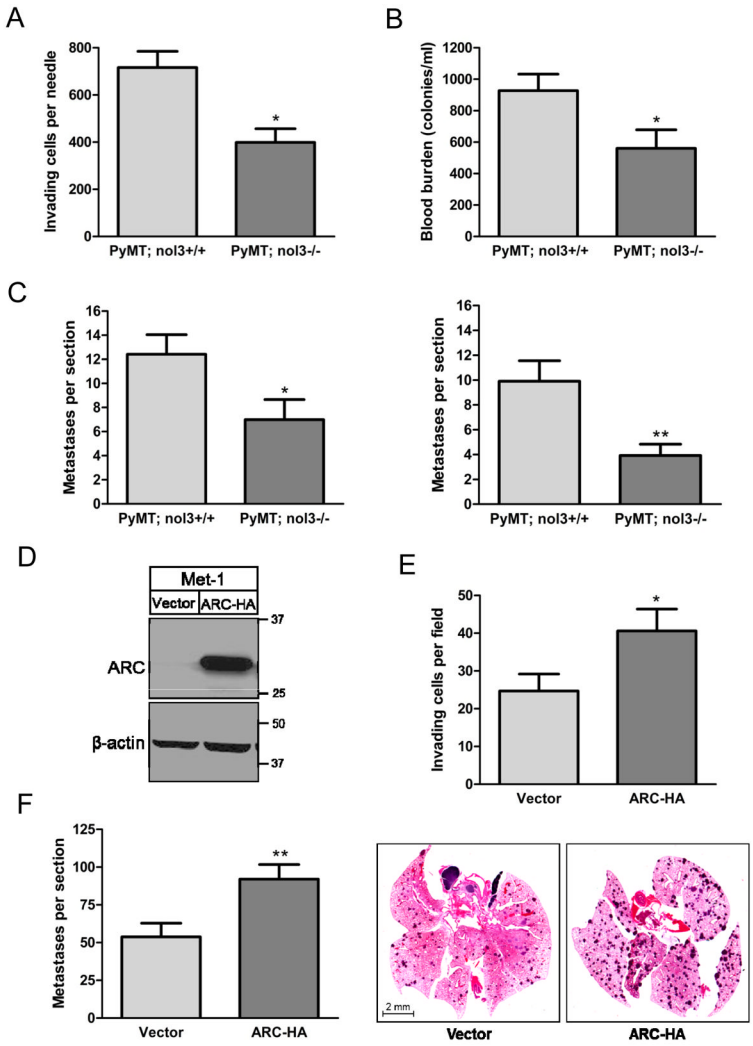

Figure 3.

ARC promotes invasion and metastasis in PyMT model. *(A) In vivo* invasion assay (see text) in PyMT mice (n = 3 *nol3*$^{+/+}$ and 3 *nol3*$^{-/-}$ mice with 6 separate needles per mouse). *(B)* Blood burden assay in PyMT mice (n = 13 *nol3*$^{+/+}$ and 10 *nol3*$^{-/-}$ mice). *(A)* and *(B)* performed on 12–14 w old mice matched for similar tumor sizes. *(C)* Left graph: Number of observable lung metastases in 14 w old PyMT mice (n = 22 *nol3*$^{+/+}$ and 26 *nol3*$^{-/-}$ mice). Analysis includes all mice regardless of tumor burden. Right graph: Number of observable lung metastases in mice with similar tumor burdens (*nol3*$^{+/+}$ 7.8 ± 0.3 g (n = 8) and *nol3*$^{-/-}$ 8.1 ± 0.2 g (n = 12); P NS). All mice with tumor burdens in the mid-range (7.0–9.0 g, see Fig. 2C) were analyzed. *(D)* Western blot for ARC in Met-1 cells stably transduced with vector or ARC-HA. *(E)* Met-1 *in vitro* invasion assay with an 8 μm PET membrane coated with Matrigel and 10% FBS as chemoattractant. (n = 4 independent experiments in triplicate with 5 fields (200×) examined per well). *(F)* Number of lung metastases 14 d following tail vein injection of Met-1 cells and representative H&E stained section showing metastases (purple) (n = 22 (vector) and 23 (ARC-HA) mice). P values: * < 0.05, ** < 0.01.

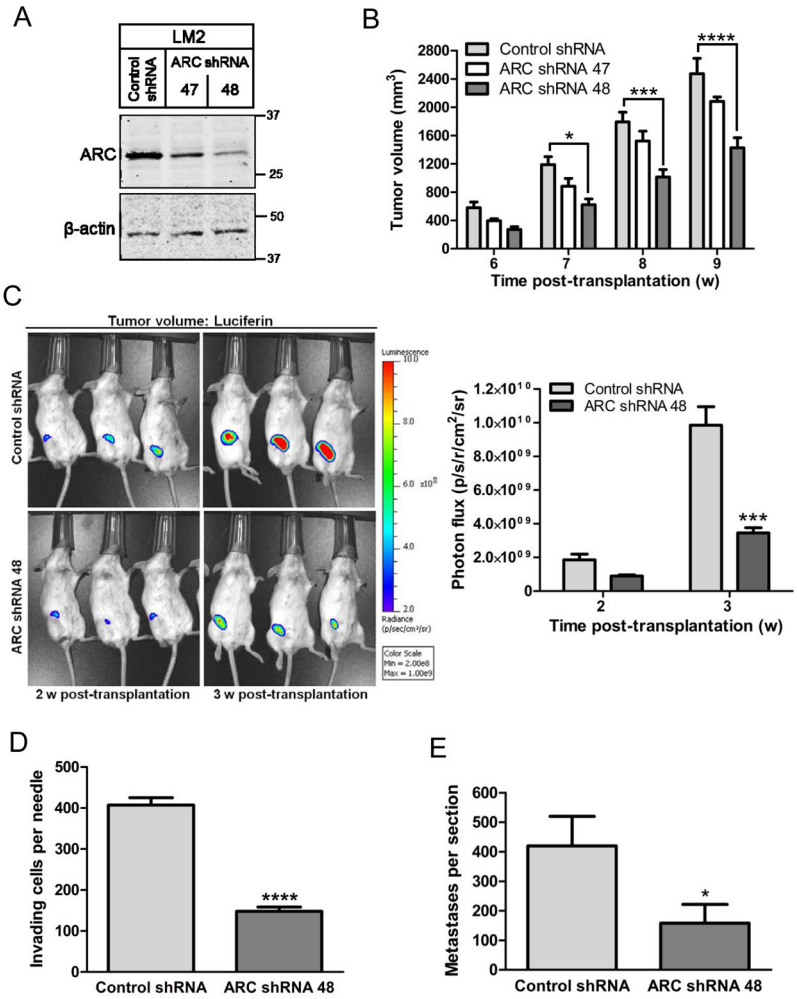

Figure 4.

ARC promotes tumorigenesis, invasion, and metastasis in mice with human LM2 mammary xenografts. *(A)* Western blot for ARC in LM2 cells stably expressing control shRNA or shRNAs targeted to ARC 3'UTR (shRNA 47) or coding region (shRNA 48). *(B)* Effect of ARC knockdown on tumor volume of LM2 xenografts as determined by caliper measurements (see Methods) (n = 15 (control shRNA), 5 (ARC shRNA 47), and 11 (ARC shRNA 48) mice). *(C)* Effect of ARC knockdown on tumor volume of LM2 xenografts at very early time points as reflected by bioluminescence (n = 7 (control shRNA) and 8 (ARC shRNA 48) mice). *(D)* Effect of ARC knockdown on *in vivo* invasion (see text) from LM2 xenografts (n = 3 (control shRNA) and 6 (ARC shRNA 48) mice). *(E)* Effect of ARC knockdown on spontaneous lung metastasis at 8 w from LM2 xenografts (n = 8 (control shRNA) and 8 (ARC shRNA 48) mice). P values: * < 0.05, *** < 0.001, **** <0.0001.

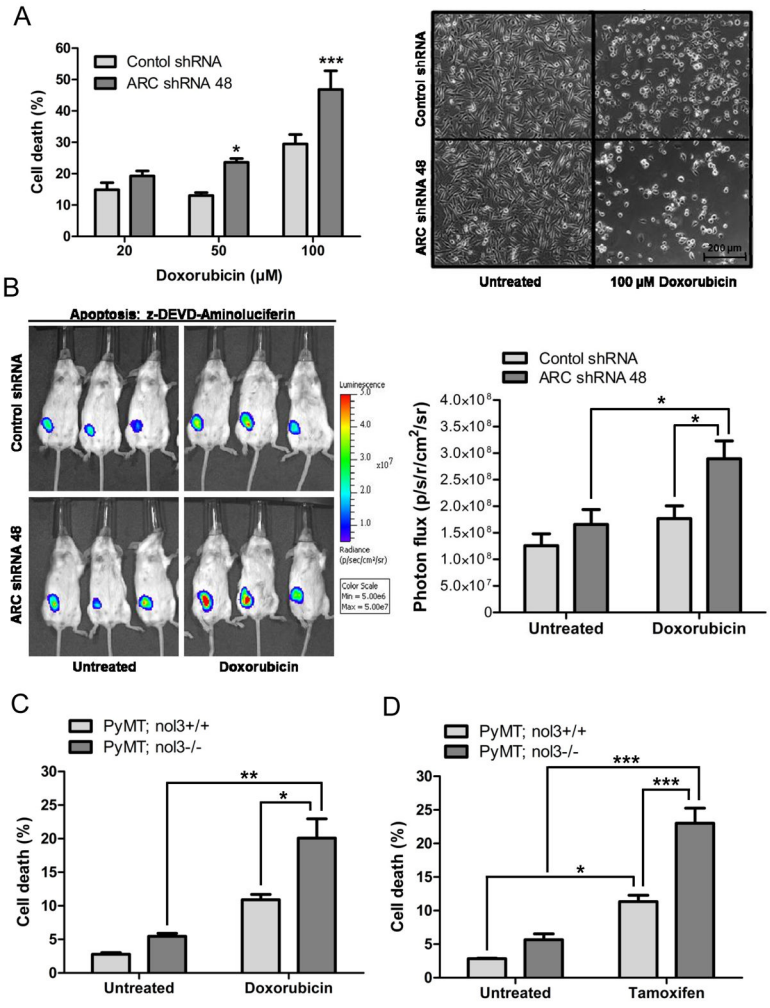

Figure 5.

Endogenous ARC levels confer chemoresistance. *(A)* Effect of ARC knockdown on sensitivity of cultured LM2 cells to killing by doxorubicin as scored by the number of ethidium bromide-positive/total cells (Hoechst 33342) (n = 2 independent experiments in triplicate, > 10 fields (200X) scored per sample) and representative phase contrast micrograph. *(B)* Effect of ARC knockdown on apoptosis in LM2 mammary xenografts 72 h post-treatment with single dose of doxorubicin (5 mg/kg ip) as measured by bioluminescence using a luciferin substrate that requires prior cleavage by endogenous caspases-3/7. (n = 8 mice in each group). (*C*) and (*D*) Sensitivity of captured invading cells from PyMT; *nol3*$^{+/+}$ and PyMT; *nol3*$^{-/-}$ mice to killing by doxorubicin (5 μM) (*C*) or tamoxifen (5 μM) (*D*) as assessed by FACS analysis of Annexin V/7-AAD stained cells. (n = 3–4 mice per group). P values: * < 0.05, ** < 0.01, *** < 0.001.